https://doi.org/10.4047/jap.2023.15.1.1

Three-dimensional morphometric analysis of facial units in virtual smiling facial images with different smile expressions

Hang-Nga Mai[1,2], Thaw Thaw Win[3], Minh Son Tong[4], Cheong-Hee Lee[3], Kyu-Bok Lee[3], So-Yeun Kim[3], Hyun-Woo Lee[5], Du-Hyeong Lee[1,3]*

[1]Institute for Translational Research in Dentistry, School of Dentistry, Kyungpook National University, Daegu, Republic of Korea
[2]Dental School of Hanoi University of business and technology, Hanoi, Vietnam
[3]Department of Prosthodontics, School of Dentistry, Kyungpook National University, Daegu, Republic of Korea
[4]School of Dentistry, Hanoi Medical University, Hanoi, Vietnam
[5]Department of Oral and Maxillofacial Surgery, Uijeongbu Eulji Medical Center, Eulji University School of Dentistry, Uijeongbu, Republic of Korea

ORCID
Hang-Nga Mai
https://orcid.org/0000-0002-9832-3312
Thaw Thaw Win
https://orcid.org/0000-0001-7460-717X
Minh Son Tong
https://orcid.org/0000-0001-8807-9101
Cheong-Hee Lee
https://orcid.org/0000-0002-2005-0801
Kyu-Bok Lee
https://orcid.org/0000-0002-1838-7229
So-Yeun Kim
https://orcid.org/0000-0001-6714-8315
Hyun-Woo Lee
https://orcid.org/0000-0002-8144-3633
Du-Hyeong Lee
https://orcid.org/0000-0003-2803-7457

Corresponding author
Du-Hyeong Lee
Department of Prosthodontics and Institute for Translational Research in Dentistry, School of Dentistry, Kyungpook National University, 2175 Dalgubeol-daero, Jung-gu, Daegu 41940, Republic of Korea
Tel +82536007676
E-mail deweylee@knu.ac.kr

Received May 20, 2022 /
Last Revision December 6, 2022 /
Accepted January 31, 2023

PURPOSE. Accuracy of image matching between resting and smiling facial models is affected by the stability of the reference surfaces. This study aimed to investigate the morphometric variations in subdivided facial units during resting, posed and spontaneous smiling. **MATERIALS AND METHODS.** The posed and spontaneous smiling faces of 33 adults were digitized and registered to the resting faces. The morphological changes of subdivided facial units at the forehead (upper and lower central, upper and lower lateral, and temple), nasal (dorsum, tip, lateral wall, and alar lobules), and chin (central and lateral) regions were assessed by measuring the 3D mesh deviations between the smiling and resting facial models. The one-way analysis of variance, Duncan post hoc tests, and Student's t-test were used to determine the differences among the groups ($\alpha = .05$). **RESULTS.** The smallest morphometric changes were observed at the upper and central forehead and nasal dorsum; meanwhile, the largest deviation was found at the nasal alar lobules in both the posed and spontaneous smiles ($P < .001$). The spontaneous smile generally resulted in larger facial unit changes than the posed smile, and significant difference was observed at the alar lobules, central chin, and lateral chin units ($P < .001$). **CONCLUSION.** The upper and central forehead and nasal dorsum are reliable areas for image matching between resting and smiling 3D facial images. The central chin area can be considered an additional reference area for posed smiles; however, special cautions should be taken when selecting this area as references for spontaneous smiles. [J Adv Prosthodont 2023;15:1-10]

KEYWORDS
Facial unit; 3D face scan; Morphometric analysis; Smile

https://doi.org/10.4047/jap.2023.15.1.1

INTRODUCTION

In the clinical practice for orthodontic, prosthodontic, and maxillofacial surgery, superimposition of multiple smiling facial images to the resting face is often required for planning, predicting, and evaluating the treatment process.[1-3] Two main image alignment methods have been introduced to merge serial three-dimensional (3D) facial images of a person, namely reference surface-based best-fit alignment and landmark point-based alignment.[4-6] Surface-based matching is reported to be superior to landmark-based matching[4,7] in terms of matching accuracy, whereas the accuracy of the surface-based image matching is significantly affected by the stability and reliability of the reference surfaces.[8,9] Anatomically, the forehead and the nose could be considered stable morphologic areas of the face in the resting state; thus, they have been commonly used as references for facial image superimposition.[8,10-12] However, there may be some differences in the subdivided facial units between spontaneous and posed smiles because of the variations in facial muscle contractions, muscle intensity, and muscle active areas when smiling.[13,14]

Generally, smile expressions can be divided into posed smiles, which are also known as the social smiles or non-Duchenne smiles, and spontaneous smiles, which are also known as enjoyment smiles or Duchenne smiles.[15] In posed smiles, only the muscles at the corners of the mouth were elevated, while in the spontaneous smile, both the muscles at the corners of the mouth and muscles orbiting the eyes are lifted.[13,15] The posed smile is a conditioned voluntary facial expression, while the spontaneous smile is an involuntary facial expression that reflects the emotion at a moment.[16,17] Posed smiles are usually more stable and consistent than spontaneous smiles.[18] Therefore, the posed or social smile is commonly used for diagnostics and treatment planning in dental and facial esthetic treatments.[19,20] However, a spontaneous smile reflects natural expressions in daily life that are missing in posed smiles; thus, obtaining spontaneous smiles is recommend to improve the quality of smile analysis.[16]

Despite suggestions on the stable reference areas for surface-based matching of 3D images of a resting face,[8,10] stable regions that keep the form in both resting and smiling expressions are still not fully elucidated.[21] Given that designation of the stable facial units during spontaneous and posed smiles may enhance the accuracy of the 3D smile facial image matching, this study aimed to investigate the morphometric variations in subdivided facial units during resting, posed, and spontaneous smiling. The null hypothesis was that there would be no morphological differences in the subdivided facial units between resting and smiling faces, regardless of the type of smiling expression (posed or spontaneous).

MATERIALS AND METHODS

This study included 33 adults (mean age, 23.5 years; range, 21 - 26 years; including 17 men and 16 women). The inclusion criteria for participant recruitment were as follows: 1) intact teeth in the anterior region and 2) facial integrity without scars that would limit natural facial expressions. The exclusion criteria were as follows: 1) participants missing anterior teeth, 2) the presence of craniofacial syndrome or malformations, 3) a history of facial trauma or maxillofacial surgery, and 4) a history of orthodontic and prosthetic treatments in the anterior region. A detailed explanation of the face scan protocol was given, and scan data were collected within regular prosthodontics education curriculum. The study design was approved by the ethical research board of Kyungpook National University Dental Hospital (KNUDH-2021-11-05-00).

3D facial scans were captured for each participant using a 3D stereophotogrammetry face scanner (RAYface 100; Ray, Seoul, Korea) equipped with multiple red, green, and blue depth (RGB-D) cameras to provide both depth and color information for the facial images. The participants were told to remove all cosmetics and facial accessories before facial scanning and to expose the forehead and ears by tightening up their hairs. During scanning, the head position and sitting posture were maintained.

Three scan acquisitions at resting, posed, and spontaneous smiles were conducted (Fig. 1). To achieve the posed smiles, the participants were asked to make a large smile while pronouncing the /e/ sound.

Spontaneous smiles were induced by suddenly showing their smile and letting them listen to a recorded laughter sound. Spontaneous smiles were verified by checking the cheek and lip corner puller muscles based on the facial action coding system (FACS).[22,23] All scans were taken following the scanner manufacturer's instructions and saved in wavefront object (OBJ) file format. Before image superimposition, unnecessary regions such as the heads and necks were eliminated from the reconstructed images.

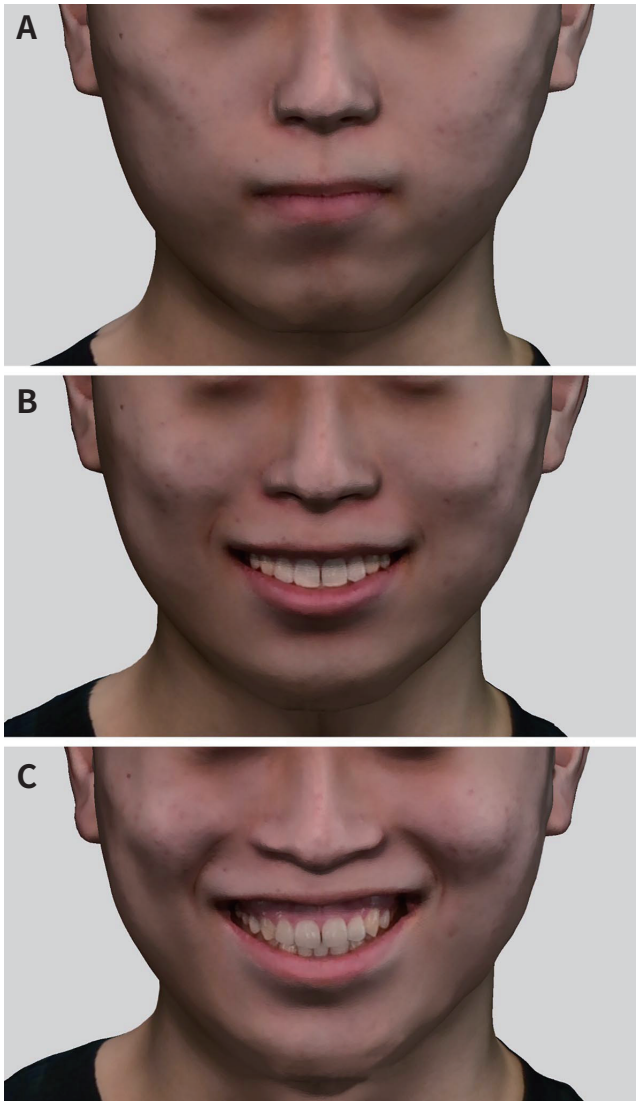

Fig. 1. Three-dimensional facial images in (A) resting position, (B) posed smile, and (C) spontaneous smile.

To access the morphometric changes in facial units, the 3D facial images of posed and spontaneous smiles were firstly aligned to those at the resting state using an image control software program (Geomagic Design X; 3D Systems, Rock Hill, SC, USA). The alignments were performed with the iterative closest point (ICP) matching algorithm, based on eight anatomic landmarks (right and left endocanthion, right and left exocanthion, glabella, pronasale, and subnasale) that showed high reproducibility on 3D facial images, according to previous studies (Fig. 2A).[24-26] The landmarks and their definitions are presented in Table 1.

In this study, the forehead, nose, and chin regions were determined by following the widely accepted facial esthetic unit definition.[27] These esthetic units were then further divided into subunits according to the principal esthetic subunits that are commonly used for facial reconstruction, plastic surgery, and dermatological treatments.[28] First, aligned facial models were cropped to include the facial region of interest, composed of the forehead, nose, and chin. Then, to overlay the cropped regions among resting and smiling images, the cropped surface model was then duplicated for selection on each subsequent model of the subdivided facial units (Fig. 2B). Accordingly, the forehead region was subdivided into five units: upper central forehead (FUC), lower central forehead (FLC), upper lateral forehead (FUL), lower lateral forehead (FLL), and temple forehead (FT). The nasal region was subdivided into four units, namely nasal dorsum (ND), nasal tip (NT), nasal lateral wall (NW), and nasal alar lobules (NL). The chin region was subdivided into two units of the central chin (CC) and lateral chin (CL). Detailed information on the facial units and subunits used is provided in Table 2.

Morphologic surface differences between resting and smiling facial models were evaluated for each of the 11 subdivided facial units using 3D surface deviation analysis. To accomplish this, the iterative closest point (ICP) algorithm of the software (Geomagic Design X) automatically matched and calculated the closest distance between point pairs on the two models. The surface-to-surface deviations between the compared facial modes at each facial unit were then visualized in a color coded map (Fig. 3) and represented as the root-mean-square error (RMSE) using the

https://doi.org/10.4047/jap.2023.15.1.1

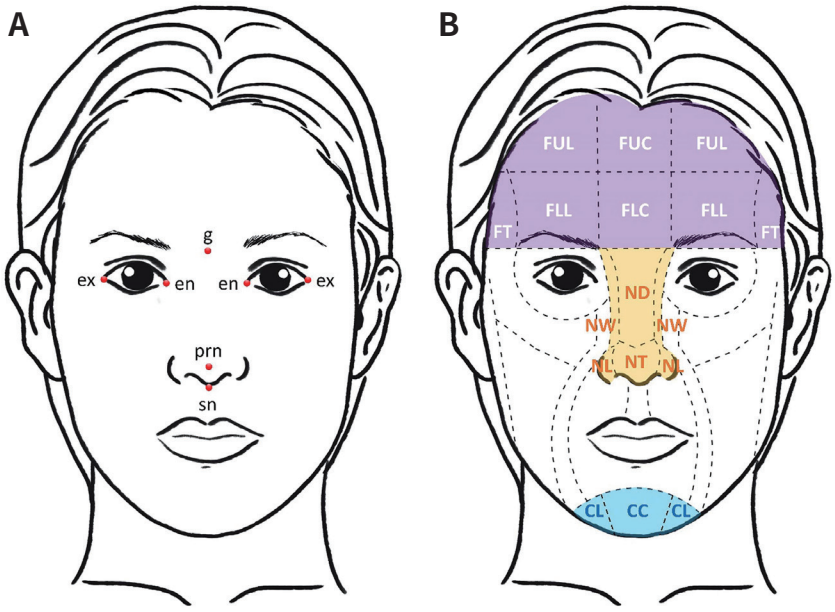

Fig. 2. Anatomical landmarks for facial image alignment and facial unit division. (A) Landmarks: glabella (g), exocanthion (ex), endocanthion (en), pronasale (prn), and subnasale (sn). (B) Facial units: upper central forehead (FUC), lower central forehead (FLC), upper lateral forehead (FUL), lower lateral forehead (FLL), temple forehead (FT), nasal dorsum (ND), nasal tip (NT), nasal lateral wall (NW), nasal alar lobules (NL), central chin (CC), and lateral chin (CL).

Table 1. Anthropometric landmarks used for facial image alignment

Landmark	Definition
Glabella (g)	The outermost midline point between the eyebrows
Exocanthion (ex)	The point at the outer commissure of the eye where the outer margin of the upper eyelid meets the lower eyelid
Endocanthion (en)	The point at the inner commissure of the eye where the inner margin of the upper eyelid meets the lower eyelid
Pronasale (prn)	The most anterior midline point of the nasal tip with the head positioned in the Frankfurt horizontal plane
Subnasale (sn)	The lowest posterior midline point at the angle formed by the outline of the nasal septum and the upper lip

Table 2. Facial units and subunits used in this study

Facial unit (boundary)	Facial subunit	Definition
Forehead (The frontal hairline superiorly, temporal hairline laterally, nasion inferomedially, and the eyebrow and glabella inferiorly)	FUC	The upper area between the medial ends of the two eyebrows
	FLC	The lower area between the medial ends of the two eyebrows
	FUL	The upper lateral area extends from the medial eyebrows to the lateral orbital rims
	FLL	The lower lateral area extends from the medial eyebrows to the lateral orbital rims
	FT	The lateral area extends from the lateral orbital rims to the zygomatic arches
Nose (The nasion superiorly, junction of the cheeks, and nasal dorsal inferiorly)	ND	The midline prominence of nose, extending from the nasal root to the nasal tip
	NT	The junction of the inferior margin of the nasal ridge and the columella
	NW	The right and left dorsal side walls
	NL	The tissue comprising the lateral boundary of the nose, inferiorly, surrounding the naris
Chin (The mentolabial fold superiorly and laterally and the lower border of the mandible inferiorly)	CC	The median area of the chin unit
	CL	The left and right areas of the chin unit

FUC, upper central forehead; FLC, lower central forehead; FUL, upper lateral forehead; FLL, lower lateral forehead; FT, temple forehead; ND, nasal dorsum; NT, nasal tip; NW, nasal lateral wall; NL, nasal alar lobules; CC, central chin; CL, lateral chin.

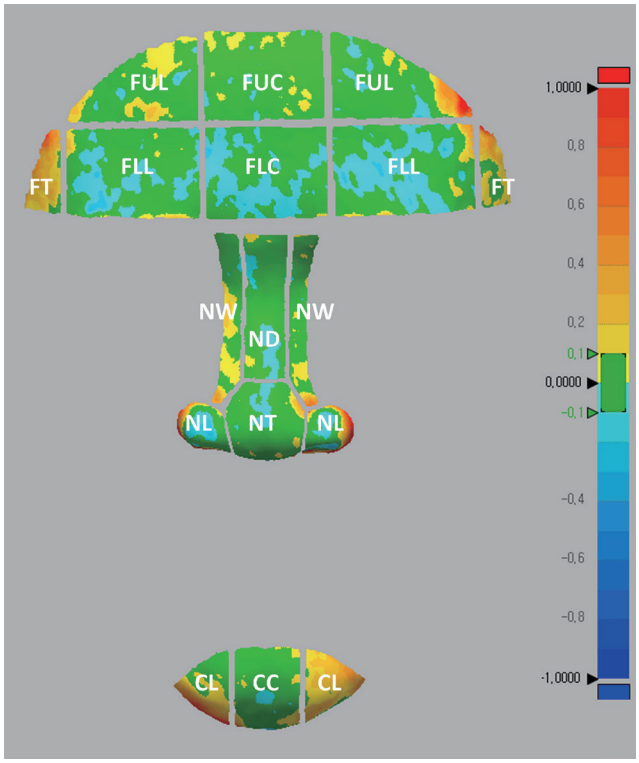

Fig. 3. Color-coded map that represented the deviations between the resting and smiling facial models at each facial unit. FUC, upper central forehead; FLC, lower central forehead; FUL, upper lateral forehead; FLL, lower lateral forehead; FT, temple forehead; ND, nasal dorsum; NT, nasal tip; NW, nasal lateral wall; NL, nasal alar lobules; CC, central chin; CL, lateral chin.

following formula:

$$\mathrm{RMSE} = \sqrt{\frac{\sum_{i=1}^{n}\left(x_{i_{test}} - x_{i_{ref}}\right)^2}{n}}$$

where $x_{i_{test}}$ is the measuring point i in the tested model, $x_{i_{ref}}$ is the paired point of point i in the reference model, and n is the total number of measuring points in the two models.

To avoid the risk of bias, all image matching, facial unit division, and mesh deviation measurements were conducted by a single experienced operator who has expertise in utilizing the image control software and was blinded to the study's purpose.

The measured RMS data on the 3D deviation of facial scans in each facial unit were calculated as mean and standard deviation. The one-way analysis of variance (ANOVA) and Duncan post hoc tests were used to determine the differences on deviation values among different facial units. To compare the facial shape between posed and spontaneous smile expressions, Student's t-test was utilized. All statistical analyses were conducted using a statistical software program (R studio version 4.1.0; R Foundation for Statistical Computing, Vienna, Austria), with statistical significance (α) at .05.

RESULTS

Table 3 shows the RMS values of 3D image deviations in the forehead, nasal, and chin facial units for both the posed and spontaneous smiles. In both the posed and spontaneous smiles, forehead units and ND unit showed significantly smaller morphometric changes than other nasal and chin units ($P < .001$). The largest deviation was observed at the facial unit of NL (0.149 ± 0.041 mm in the posed smile and 0.193 ± 0.060 mm in the spontaneous smile) ($P < .001$).

Subregional analyses of the facial units at different facial regions are presented in Figure 4. In the forehead, the temple unit showed significantly higher morphometric changes than other forehead units. In the nasal region, the dorsum unit exhibited the lowest morphometric change, followed by the lateral wall, tip, and alar lobules units. Meanwhile, in the chin region, no difference was found on the morphometric change between the central and lateral units.

A comparison of the facial images obtained with different smile expressions revealed no significant morphometric changes in the forehead and nasal regions in general. However, significant changes were found between smile expressions in the alar lobules, CC, and CL facial units ($P < .05$) (Fig. 5).

DISCUSSION

This study investigated morphometric changes of facial units during smiling expressions and evaluated the variation of these facial units in 3D facial images of posed and spontaneous smiles. In both posed and spontaneous smiles, the low morphometric changes were shown at the upper and center units of the forehead and dorsum unit of the nasal region, and

https://doi.org/10.4047/jap.2023.15.1.1

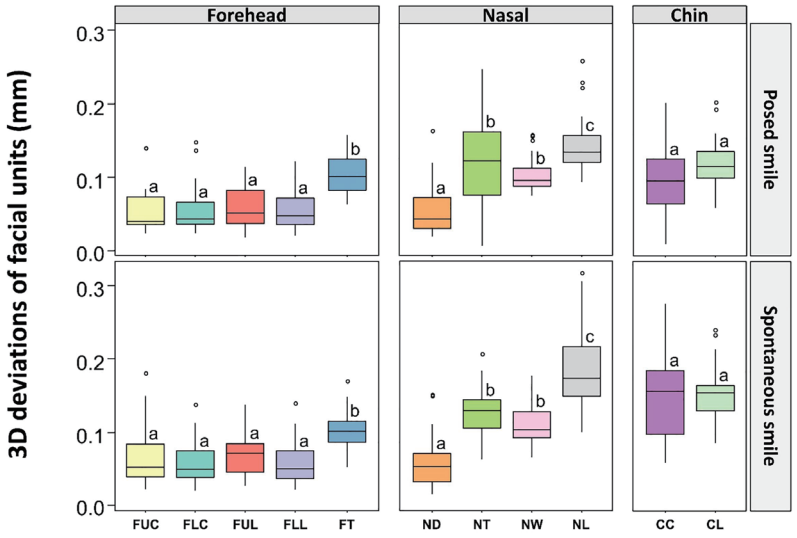

Fig. 4. Three-dimensional deviations of the posed and spontaneous smiling facial models from the resting facial models at each facial unit. Different letters indicate a significant difference between 3D deviation of facial scan at each facial unit ($P < .05$). FUC, upper central forehead; FLC, lower central forehead; FUL, upper lateral forehead; FLL, lower lateral forehead; FT, temple forehead; ND, nasal dorsum; NT, nasal tip; NW, nasal lateral wall; NL, nasal alar lobules; CC, central chin; CL, lateral chin.

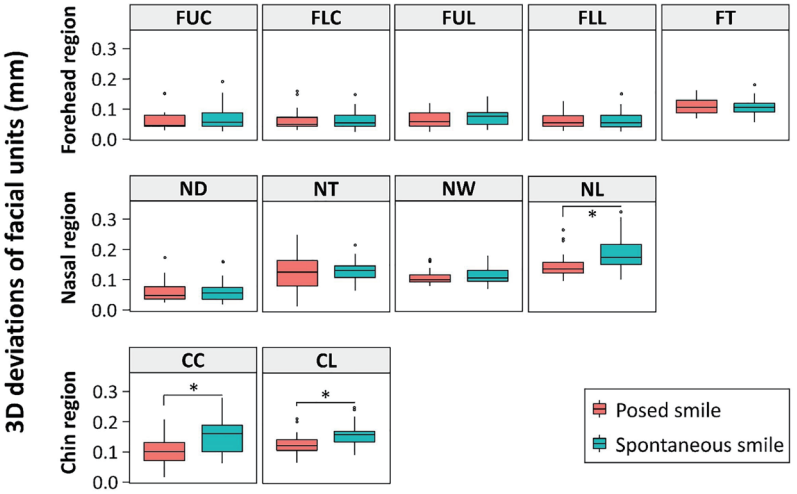

Fig. 5. Variations between resting and smiling facial models at each facial unit.
*Significant difference.
FUC, upper central forehead; FLC, lower central forehead; FUL, upper lateral forehead; FLL, lower lateral forehead; FT, temple forehead; ND, nasal dorsum; NT, nasal tip; NW, nasal lateral wall; NL, nasal alar lobules; CC, central chin; CL, lateral chin.

Table 3. Three-dimensional deviations of the posed and spontaneous smiles from the resting face at various facial units

Facial region	Facial units	Posed smile Mean (SD) (mm)	Spontaneous smile Mean (SD) (mm)	*P*-value
Forehead	Upper central	0.062 (0.032)^{a}	0.063 (0.029)^{a}	.434
	Lower central	0.063 (0.030)^{a}	0.072 (0.039)^{a}	.898
	Upper lateral	0.064 (0.026)^{a}	0.063 (0.029)^{a}	.475
	Lower lateral	0.067 (0.027)^{a}	0.074 (0.03)^{a}	.978
	Temple	0.108 (0.027)^{b}	0.108 (0.027)^{b}	.979
Nasal	Dorsum	0.063 (0.035)^{a}	0.063 (0.036)^{a}	.970
	Tip	0.121 (0.062)^{b}	0.133 (0.036)^{c,d}	.288
	Lateral wall	0.110 (0.023)^{b}	0.116 (0.030)^{b,c}	.573
	Alar lobules	0.149 (0.041)^{c,1}	0.193 (0.060)^{f,2}	< .001
Chin	Central	0.102 (0.053)^{b,1}	0.152 (0.058)^{d,e,2}	< .001
	Lateral	0.124 (0.035)^{b,1}	0.178 (0.037)^{e,2}	.010
	P-value	< .001	< .001	

Different superscript letters in the same column indicate a significant difference between facial units; different superscript numbers in the same row indicate a significant difference between the posed and spontaneous smiles ($P < .05$). SD: Standard deviation.

high morphometric changes were found at the alar lobule unit of the nasal and lateral unit of the chin. Subregional analyses of facial units at different facial regions showed significant differences between the morphometric changes of facial units at the forehead and nasal regions, whereas no significant difference was noted between the two units at the chin region. Meanwhile, a comparison of the facial images obtained with different smile postures revealed that the spontaneous smile generally resulted in larger facial unit changes than did the posed smile, with a significant difference observed at the alar lobules, central chin, and lateral chin units. Thus, the null hypothesis of this study was rejected.

The stability of the reference matching surfaces is a vital factor for the accuracy of the 3D facial image matching.[10,19,20,29] In the literature, landmarks at the forehead and nasal region and the whole surface of the forehead and nasal region have been commonly selected as references for 3D facial image superimposition because of their stable anatomic morphology.[8,10-12] However, variations within the forehead, nasal region of the same individual have been reported.[10] In addition, the image matching accuracy was reported to be dependent on the use of different areas of the forehead and nasal regions as references for image matching.[8] In this study, morphometric changes in facial subunits were significantly different at the forehead and nasal region for both the posed and spontaneous smiles.

At the forehead, higher morphometric changes were observed at the lower and lateral units than in the upper and central units. The possible reason was the higher myogenic potential changes that occurred at the lower forehead area of bilateral muscles, such as the frontalis, corrugator, and depressor supercilii, which are responsible for the movements around the eyebrow during facial expressions, than in the upper forehead area.[30] At the nasal region, the dorsum unit exhibited the lowest morphometric changes, followed by the lateral wall, tip, and alar lobules. The results were corresponding well with the anatomical activities of facial muscles during smiles.[31] Accordingly, the greater deformity of the nasal tip and alar lobules was caused by the action of the depressor septi nasi muscle, which depresses the nasal tip and widens the alar lobules.[32,33] This muscle is formed by three fascicle groups: medial fascicles that start from the anterior nasal spine and attach to the upper lip, intermediate fascicles that connect the medial and lateral fascicles, and lateral fascicles that originate from the maxilla and attach to the alar cartilage.[34] Because of the medial fascicles, the movement of the upper lip during smiling has a significant effect on the changes of the nasal base that consists of the nasal alar flaring and nasal tip depression.[32]

Although the forehead and nasal region have been commonly used as references for facial image matching, the two regions are located toward the upper parts of the face. Previous studies have reported that even distribution of the reference points may enhance the accuracy of 3D image matching.[35,36] Thus, the addition of the chin area that is located in the lower part of the face is expected to be providing more even distribution of the reference surfaces for image matching. However, a previous study that assessed the morphological and metrical modifications of 3D facial images in the different facial expressions revealed that the most evident changes were observed in the mouth and chin regions, particularly with smiling expressions.[24] Based on this study's results, the center chin area might be considered an additional reference area for posed smiles; however, caution should be taken when using the chin area as a reference surface for matching spontaneous smile facial images.

The significant differences between the spontaneous and posed smiling images in terms of the alar lobules, central chin, and lateral chin units may be explained by the differences in facial muscle movements that occur during smiling. A comparative study of lip position during spontaneous and posed smiling in adults reported that both the lip-line height and smile width during spontaneous smiling were significantly higher than during posed smiling, which imply the higher movement range of the lip muscles during spontaneous smile than during posed smile.[37] As the upper lip muscle has a significant effect on the position of the nasal base,[32] the differences in lip movement range during spontaneous and posed smiling further explains why spontaneous smiles resulted in significantly larger morphometric changes of the alar lobule unit than posed smiles. Interestingly, sig-

https://doi.org/10.4047/jap.2023.15.1.1

nificantly higher morphometric changes in the center and lateral chin subunits were observed in spontaneous smiles in comparison to posed smiles. This could be attributed to the fact that the chin muscles that respond to lower lip movements, such as the mentalis and depressor labii inferioris, are more relaxed during spontaneous smiles than during posed smiles.

In this study, facial images were captured using an RGB-D stereophotogrammetric facial scanner that can provide high-resolution 3D facial images with both depth and color information. This type of facial scanner has been reported to be accurate and reliable for facial scanning in dental treatment.[38-41] With the advancement in the capabilities and reliability of 3D facial scanners, the use of integrating 3D facial images in a digital workflow to create a virtual patient for advanced prosthodontic treatment has increased rapidly.[42-46] For accurate image superimposition in clinical situations, where the alignment of a series of 3D facial images is required, it is essential to find a reliable matching strategy for the images. Although previous studies have suggested reference surface areas for 3D image matching,[8,10-12] standards for selecting the exact size and position of these reference areas have not been reported. Uncertainties in selecting a reliable reference surface for 3D facial image matching may affect the accuracy of the matching. Because of this, the findings of this study may assist clinicians in selecting reliable reference surface areas for accurate 3D image matching between resting and smiling faces, allowing for better diagnosis, treatment planning, and prognosis.

The limitations of this study are related to the restrictions in age and ethnicity of the sample group. In addition, factors on operator-related characteristics were excluded, such as the operator's knowledge and skill in utilizing image control software for 3D image matching. Further research on varied face types and shapes of people of various ages and ethnicities should be considered to expand the implications of this study. Future studies should address the effect of operator-related variables.

CONCLUSION

The upper and central units of the forehead and dorsum unit of the nasal region exhibited the smallest morphometric changes during both the posed and spontaneous smiles; thus, they are reliable areas for image matching between resting and smiling 3D facial images. The central chin area can be considered an additional reference area when posed smiles are matched. In the spontaneous smile, the morphometric changes of the nasal alar lobules and chin areas are significantly large compared with the changes in the posed smile; therefore, special cautions should be taken when selecting these areas as image matching references for spontaneous smile facial images.

REFERENCES

1. Pucciarelli V, Gibelli D, Barni L, Gagliano N, Dolci C, Sforza C. Assessing normal smiling function through 3D-3D surfaces registration: an innovative method for the assessment of facial mimicry. Aesthetic Plast Surg 2018;42:456-63.
2. Demir R, Baysal A. Three-dimensional evaluation of smile characteristics in subjects with increased vertical facial dimensions. Am J Orthod Dentofacial Orthop 2020;157:773-82.
3. Horn S, Matuszewska N, Gkantidis N, Verna C, Kanavakis G. Smile dimensions affect self-perceived smile attractiveness. Sci Rep 2021;11:2779.
4. Wampfler JJ, Gkantidis N. Superimposition of serial 3-dimensional facial photographs to assess changes over time: A systematic review. Am J Orthod Dentofacial Orthop 2022;161:182-97.e2.
5. Maal TJ, van Loon B, Plooij JM, Rangel F, Ettema AM, Borstlap WA, Bergé SJ. Registration of 3-dimensional facial photographs for clinical use. J Oral Maxillofac Surg 2010;68:2391-401.
6. Naros A, Wolf JA, Krimmel M, Kluba S. Three-dimensional quantification of facial asymmetry in children with positional cranial deformity. Plast Reconstr Surg 2021;148:1321-31.
7. Gkantidis N, Schauseil M, Pazera P, Zorkun B, Katsaros C, Ludwig B. Evaluation of 3-dimensional superimposition techniques on various skeletal structures of the head using surface models. PLoS One 2015;10:

e0118810.
8. Häner S, Kanavakis G, Matthey F, Gkantidis N. Valid 3D surface superimposition references to assess facial changes during growth. Sci Rep 2021;11:16456.
9. Cammarata MJ, Wake N, Kantar RS, Maroutsis M, Rifkin WJ, Hazen A, Brecht LE, Bernstein GL, Diaz-Siso JR, Rodriguez ED. Three-dimensional analysis of donor masks for facial transplantation. Plast Reconstr Surg 2019;143:1290e-7e.
10. Maal TJ, Verhamme LM, van Loon B, Plooij JM, Rangel FA, Kho A, Bronkhorst EM, Bergé SJ. Variation of the face in rest using 3D stereophotogrammetry. Int J Oral Maxillofac Surg 2011;40:1252-7.
11. Altındiş S, Toy E, Başçiftçi FA. Effects of different rapid maxillary expansion appliances on facial soft tissues using three-dimensional imaging. Angle Orthod 2016;86:590-8.
12. van der Meer WJ, Dijkstra PU, Visser A, Vissink A, Ren Y. Reliability and validity of measurements of facial swelling with a stereophotogrammetry optical three-dimensional scanner. Br J Oral Maxillofac Surg 2014;52:922-7.
13. Park S, Lee K, Lim JA, Ko H, Kim T, Lee JI, Kim H, Han SJ, Kim JS, Park S, Lee JY, Lee EC. Differences in facial expressions between spontaneous and posed smiles: automated method by action units and three-dimensional facial landmarks. Sensors (Basel) 2020;20:1199.
14. Lambros V. Facial aging: a 54-year, three-dimensional population study. Plast Reconstr Surg 2020;145:921-8.
15. Manjula WS, Sukumar MR, Kishorekumar S, Gnanashanmugam K, Mahalakshmi K. Smile: a review. J Pharm Bioallied Sci 2015;7:S271-5.
16. Ekman P, Friesen WV. Felt, false, and miserable smiles. J Nonverbal Behav 1982;6:238–52.
17. Lin Y, Lin H, Lin Q, Zhang J, Zhu P, Lu Y, Zhao Z, Lv J, Lee MK, Xu Y. A novel three-dimensional smile analysis based on dynamic evaluation of facial curve contour. Sci Rep 2016;6:22103.
18. Hulsey CM. An esthetic evaluation of lip-teeth relationships present in the smile. Am J Orthod 1970;57:132-44.
19. Dindaroğlu F, Duran GS, Görgülü S, Yetkiner E. Social smile reproducibility using 3-D stereophotogrammetry and reverse engineering technology. Angle Orthod 2016;86:448-55.
20. Tanikawa C, Takada K. Test-retest reliability of smile tasks using three-dimensional facial topography. Angle Orthod 2018;88:319-28.
21. Rudy HL, Wake N, Yee J, Garfein ES, Tepper OM. Three-dimensional facial scanning at the fingertips of patients and surgeons: accuracy and precision testing of iPhone X three-dimensional scanner. Plast Reconstr Surg 2020;146:1407-17.
22. Clark EA, Kessinger J, Duncan SE, Bell MA, Lahne J, Gallagher DL, O'Keefe SF. The facial action coding system for characterization of human affective response to consumer product-based stimuli: a systematic review. Front Psychol 2020;11:920.
23. Gunnery SD, Ruben MA. Perceptions of Duchenne and non-Duchenne smiles: A meta-analysis. Cogn Emot 2016;30:501-15.
24. Gibelli D, De Angelis D, Poppa P, Sforza C, Cattaneo C. An assessment of how facial mimicry can change facial morphology: implications for identification. J Forensic Sci 2017;62:405-10.
25. Cummaudo M, Guerzoni M, Marasciuolo L, Gibelli D, Cigada A, Obertovà Z, Ratnayake M, Poppa P, Gabriel P, Ritz-Timme S, Cattaneo C. Pitfalls at the root of facial assessment on photographs: a quantitative study of accuracy in positioning facial landmarks. Int J Legal Med 2013;127:699-706.
26. Othman SA, Ahmad R, Mericant AF, Jamaludin M. Reproducibility of facial soft tissue landmarks on facial images captured on a 3D camera. Aust Orthod J 2013;29:58-65.
27. Fattahi TT. An overview of facial aesthetic units. J Oral Maxillofac Surg 2003;61:1207-11.
28. Ilankovan V, Ethunandan M, Seah TE. Facial units and subunits. In: Local flaps in facial reconstruction. 1st ed. Cham: Springer International Publishing;, 2015. p. 23-43.
29. Yamamoto S, Miyachi H, Fujii H, Ochiai S, Watanabe S, Shimozato K. Intuitive facial imaging method for evaluation of postoperative swelling: a combination of 3-dimensional computed tomography and laser surface scanning in orthognathic surgery. J Oral Maxillofac Surg 2016;74:2506.e1-10.
30. Kuramoto E, Yoshinaga S, Nakao H, Nemoto S, Ishida Y. Characteristics of facial muscle activity during voluntary facial expressions: Imaging analysis of facial expressions based on myogenic potential data. Neuropsychopharmacol Rep 2019;39:183-93.

31. Schumann NP, Bongers K, Scholle HC, Guntinas-Lichius O. Atlas of voluntary facial muscle activation: Visualization of surface electromyographic activities of facial muscles during mimic exercises. PLoS One 2021; 16:e0254932.
32. Beiraghi-Toosi A, Rezaei E, Zanjani E. Relationship between hyperactivity of depressor septi nasi muscle and changes of alar base and flaring during smile. World J Plast Surg 2016;5:45-50.
33. Standring S, Ellis H, Healy J, Johnson D, Williams A, Collins P, Wigley C. Gray's anatomy: the anatomical basis of clinical practice. AJNR Am J Neuroradiol 2005;26:2703.
34. De Souza Pinto EB, Da Rocha RP, Filho WQ, Neto ES, Zacharias KG, Amâncio A, Braz de Camargo A. Anatomy of the median part of the septum depressor muscle in aesthetic surgery. Aesthetic Plast Surg 1998;22: 111-5.
35. Mai HY, Lee DH. Impact of matching point selections on image registration accuracy between optical scan and computed tomography. Biomed Res Int 2020; 2020:3285431.
36. Choi YD, Mai HN, Mai HY, Ha JH, Li LJ, Lee DH. The effects of distribution of image matched fiducial markers on accuracy of computer-guided implant surgery. J Prosthodont 2020;29:409-14.
37. Van Der Geld P, Oosterveld P, Berge SJ, Kuijpers-Jagtman AM. Tooth display and lip position during spontaneous and posed smiling in adults. Acta Odontol Scand 2008;66:207-13.
38. Dindaroğlu F, Kutlu P, Duran GS, Görgülü S, Aslan E. Accuracy and reliability of 3D stereophotogrammetry: A comparison to direct anthropometry and 2D photogrammetry. Angle Orthod 2016;86:487-94.
39. Liu J, Zhang C, Cai R, Yao Y, Zhao Z, Liao W. Accuracy of 3-dimensional stereophotogrammetry: Comparison of the 3dMD and Bellus3D facial scanning systems with one another and with direct anthropometry. Am J Orthod Dentofacial Orthop 2021;160:862-71.
40. Pan F, Liu J, Cen Y, Chen Y, Cai R, Zhao Z, Liao W, Wang J. Accuracy of RGB-D camera-based and stereophotogrammetric facial scanners: a comparative study. J Dent 2022;127:104302.
41. D'Ettorre G, Farronato M, Candida E, Quinzi V, Grippaudo C. A comparison between stereophotogrammetry and smartphone structured light technology for three-dimensional face scanning. Angle Orthod 2022;92:358-63.
42. Hassan B, Greven M, Wismeijer D. Integrating 3D facial scanning in a digital workflow to CAD/CAM design and fabricate complete dentures for immediate total mouth rehabilitation. J Adv Prosthodont 2017;9:381-6.
43. Lin WS, Harris BT, Phasuk K, Llop DR, Morton D. Integrating a facial scan, virtual smile design, and 3D virtual patient for treatment with CAD-CAM ceramic veneers: A clinical report. J Prosthet Dent 2018;119:200-5.
44. Daher R, Ardu S, Vjero O, Krejci I. 3D digital smile design with a mobile phone and intraoral optical scanner. Compend Contin Educ Dent 2018;39:e5-e8.
45. Park JM, Oh KC, Shim JS. Integration of intraoral digital scans with a 3D facial scan for anterior tooth rehabilitation. J Prosthet Dent 2019;121:394-7.
46. Jreige CS, Kimura RN, Segundo ÂRTC, Coachman C, Sesma N. Esthetic treatment planning with digital animation of the smile dynamics: A technique to create a 4-dimensional virtual patient. J Prosthet Dent 2022; 128:130-8.